JACS
JOURNAL OF THE AMERICAN CHEMICAL SOCIETY
pubs.acs.org/JACS
Article

Dearomative Skeletal Editing of Benzenoids via Diradical

Xiang-Xin Zhang, Shan-Tong Xu, Xue-Ting Li, Ting-Ting Song, Ding-Wei Ji, and Qing-An Chen*

Cite This: J. Am. Chem. Soc. 2025, 147, 11533−11542
Read Online
ACCESS | Metrics & More | Article Recommendations | Supporting Information

ABSTRACT: Dearomative skeletal editing of benzenoids represents a promising yet challenging strategy for the rapid construction of high-value carbon frameworks from readily accessible starting materials. Büchner reaction is a unique type of expansive skeletal editing that transforms benzenoids into functionalized cycloheptatrienes. However, due to challenges in compatibility and selectivity, achieving seamless integration of this reaction with dearomative cycloaddition within a unified system remains undeveloped. Here, we demonstrated an energy-transfer-induced intermolecular dearomative skeletal editing reaction of benzenoids with a range of electronically diverse alkynes. This protocol employed *N*-acylimines as diradical precursors to efficiently construct various structurally diverse polycyclic frameworks in high chemo-, regio-, and diastereoselectivities that have been previously inaccessible. The challenges related to general reactivity and selectivity issues were circumvented through the smooth merging of photoinduced skeletal editing with dearomative cycloaddition. Experimental and computational studies were performed to support the diradical mechanism and interpret the origins of the observed chemo-, regio-, and diastereoselectivities.

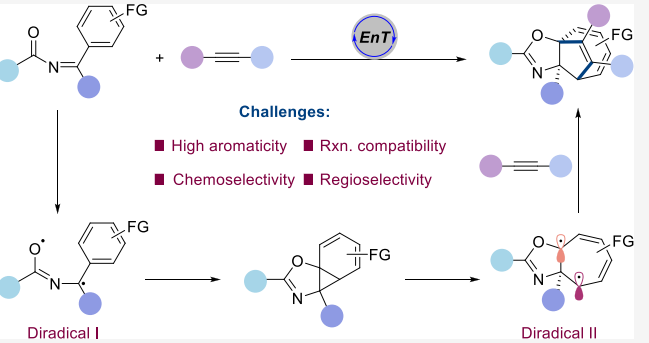

INTRODUCTION

As bulk and fundamental chemical feedstocks, benzenoids play important roles in chemistry, materials, medicines, etc. Due to its inherent aromaticity,[1] the delocalization of the π-electrons makes it particularly stable, and hence, many approaches to benzenoid transformations are concentrated in the functionalization of peripheral C−H or C−X bonds (Figure 1A).[2] Recently, the "escape from flatland" concept,[3] which transforms planar aromatic rings into three-dimensional (3D) scaffolds, has become a key strategy in modern drug discovery for optimizing molecular properties and enhancing target interactions. Notably, dearomatization has become an increasing cornerstone of the synthetic methodology, serving as a critical tactic for disrupting molecular planarity.[4] Uniquely, dearomative cycloaddition emerges as a powerful and economical strategy for the efficient conversion of simple arenes into unprecedentedly diverse polycyclic scaffolds.[4a,5] However, overcoming the aromatic stability of these conjugated systems poses significant kinetic and thermodynamic challenges.[6] Therefore, it is of great interest to develop efficient strategies for the construction of complex three-dimensional molecules from simple two-dimensional planar molecules.

In recent decades, the rapid development of photocatalysis, particularly energy transfer catalysis (EnT),[7] has enabled the efficient transformation of traditionally unreactive substrates into valuable products via radical intermediates under mild conditions. Remarkably, significant progress has been achieved in visible light-promoted catalytic dearomative cycloaddition.[8] Intermolecular cycloadditions of benzene rings with unsaturated partners can yield *ortho*-, *meta*-, and *para*-regioisomers in terms of topology[5,9] (Figure 1B). For example, Glorius[10] and You[11] groups have independently realized photocatalytic dearomatization reactions of (hetero-) fused arenes via [2+2] or [4+2] cycloaddition, respectively. The *meta*-cycloaddition of benzene rings[9] usually necessitates high-energy ultraviolet (UV) light. Due to the higher aromaticity of benzenoids compared to fused-ring compounds, most dearomative cycloaddition of benzene rings focuses on ring-fused aromatic compounds. Therefore, it is of great challenge to develop an intermolecular dearomative cycloaddition of nonfused benzene rings.

In traditional dearomative cycloaddition, the original carbon skeletons of benzenoids were maintained (Figure 1C). Single-atom skeletal editing[12] provides a mild and selective approach for the site-directed mutagenesis of molecular frameworks. The seamless integration of skeletal editing and dearomative cycloaddition offers a powerful strategy to greatly enhance molecular structural diversity, unlocking a broader application

Received: February 2, 2025
Revised: March 12, 2025
Accepted: March 13, 2025
Published: March 25, 2025

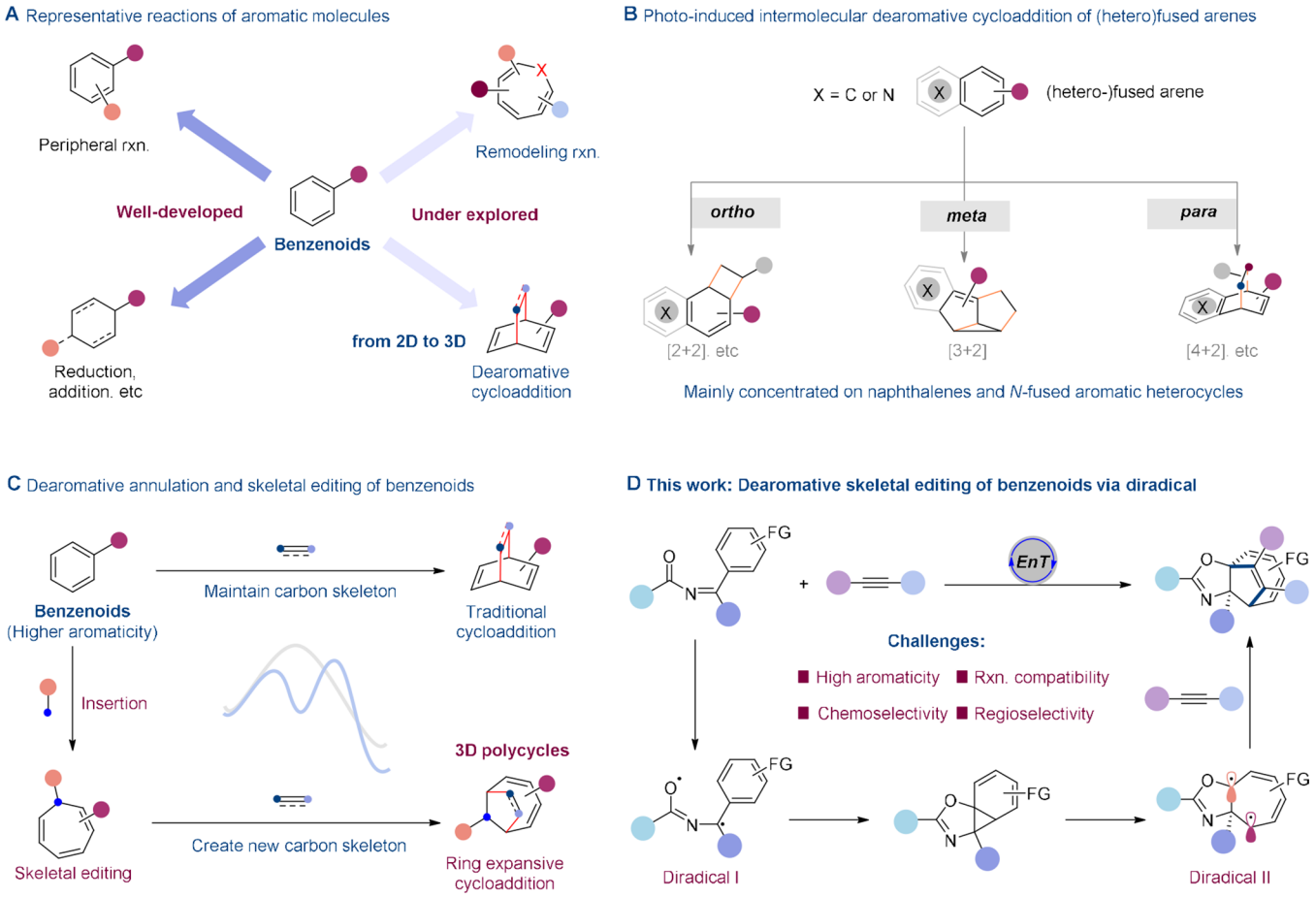

Figure 1. Approaches to polycyclic structures through dearomative skeletal editing of benzenoids.

potential for aromatic compounds. As a unique type of expansive skeletal editing, the Büchner reaction has become a practical and effective strategy for directly constructing valuable functionalized cycloheptatrienes (CHTs) from simple aromatic precursors.[13] Therefore, combining the Büchner reaction with dearomative cycloaddition could potentially yield polycyclic compounds distinct from conventional cycloaddition products. Owing to the inherent limitations of carbene or nitrene precursors,[13,14] most efforts have primarily focused on generating the corresponding CHTs and azepines. Meanwhile, the equilibrium between the norcaradiene (NCD) and CHT[15] introduces significant challenges to achieving intermolecular cycloaddition, encompassing chemo-, regio-, and diastereoselectivity.

Given the electronic structure (two unshared valence electrons on the same carbon) of carbenes, we wondered whether the diradical precursors (two unpaired valence electrons on different atoms) could give us new opportunities in skeletal editing of benzenoids (Figure 1D). Based on their unique structural property and our previous experience in photocatalysis,[16] we thought *N*-acylimine could serve as a novel and atom-economic diradical precursor to facilitate a cascade dearomative skeletal editing and cycloaddition through generating the CHT diradical under EnT. However, the presence of various potential diradicals (Figure S2) could cause counterproductive side reactions with radical receptors (Figure S3). By addressing the associated challenges (high aromaticity of benzenoids, reaction compatibility, chemo-, and regioselective control), we herein developed a photochemical dearomative skeletal editing of benzenoids with alkynes under EnT, enabling the construction of complex three-dimensional polycyclic skeletons by a diradical (Figure 1D).

RESULTS AND DISCUSSION

Reaction Optimization. In the initial stage of the reaction investigation, various potential radical acceptors were explored (Figure S4). However, apart from alkynes, all other attempts encountered compatibility issues. Many of these failed to yield the desired products or faced challenges in diastereoselectivity (e.g., for styrene, dr = 2:1). Subsequently, we began our investigation with the use of *N*-(diphenylmethylene) benzamide (**1a**) and ethyl 3-phenylpropiolate (**2a**) as reaction partners (Table S1 in the Supporting Information). After careful optimization, tricyclo[4.4.2.0^{1,5}] product **3** was obtained in 76% isolated yield under standard conditions with **PC-1** (2-chloro-9*H*-thioxanthen-9-one) as a photocatalyst with good chemo- and regioselectivity (entry 1, Table S1). The effect of other reaction parameters on aromatic dearomative skeletal editing was further evaluated. Varying the wavelength of the reaction greatly decreased the yields (entry 2, Table S1). Moreover, through the investigation of photocatalysts, only Ir[dF(CF$_3$)ppy]$_2$[dtbbpy]PF$_6$, Ir(dF-ppy)$_3$, **PC-1**, and its derived photocatalysts could promote the desired dearomative skeletal editing (entries 3−5 and Table S1 in the Supporting Information). Additionally, other solvents, such as ethyl acetate (EA), dichloromethane (DCM), methanol (MeOH), and dimethyl sulfoxide (DMSO), led to a substantial decrease in reaction yields (entries 6−10, Table S1). Changing different

https://doi.org/10.1021/jacs.5c01983
J. Am. Chem. Soc. 2025, 147, 11533−11542

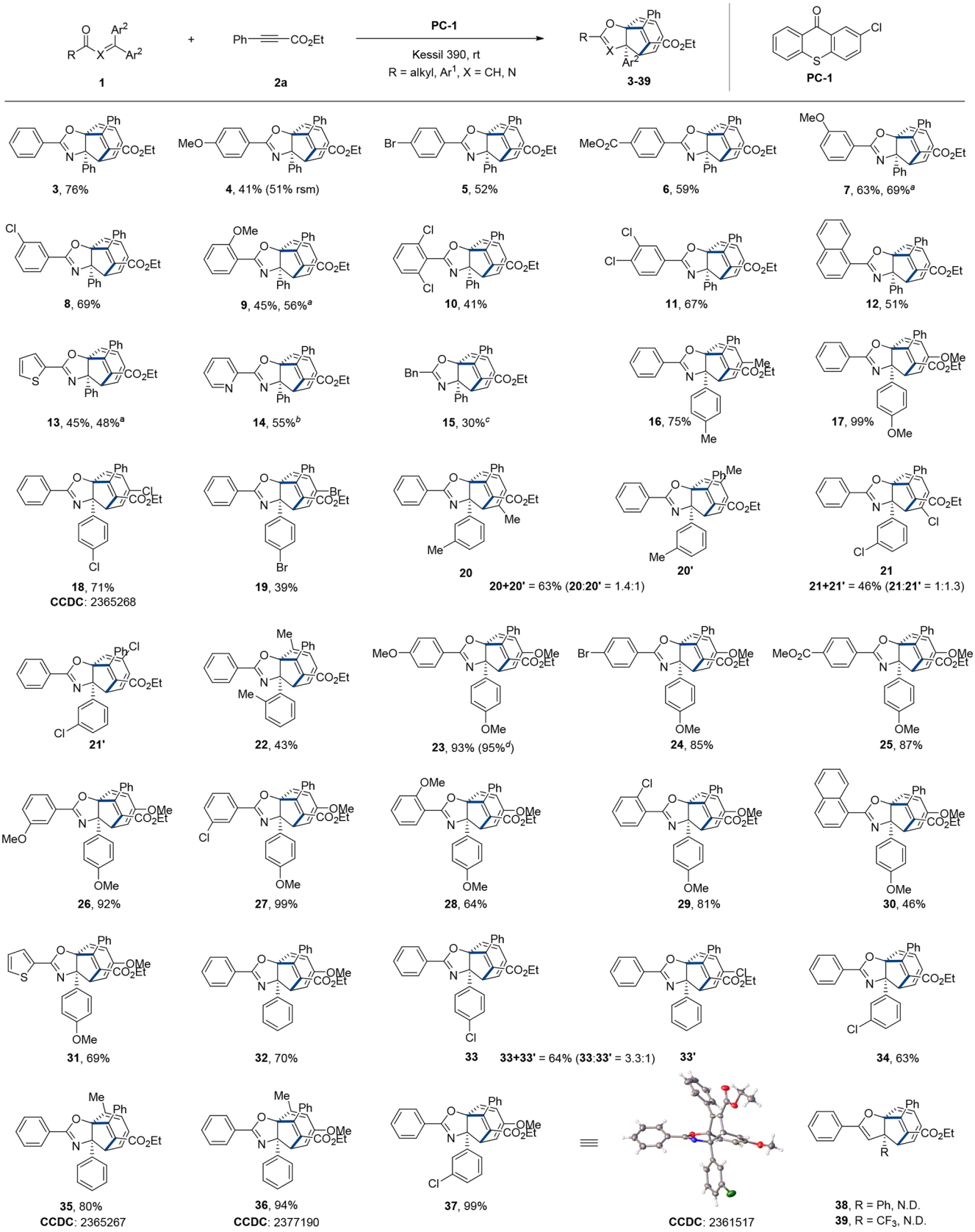

Figure 2. Substrate scope of *N*-acylimines. Conditions: **1** (0.20 mmol), **2a** (0.50 mmol), **PC-1** (0.04 mmol), $ZnCl_2$ (0.20 mmol), MeCN (0.5 mL), Kessil 390 nm, 40 W, room temperature, 24 h. Isolated yields were given; [a]48 h; [b]No $ZnCl_2$, MeCN: DCM = 1:1 (0.5 mL); [c]365 nm, 50 W; [d]No $ZnCl_2$.

https://doi.org/10.1021/jacs.5c01983
J. Am. Chem. Soc. 2025, 147, 11533−11542

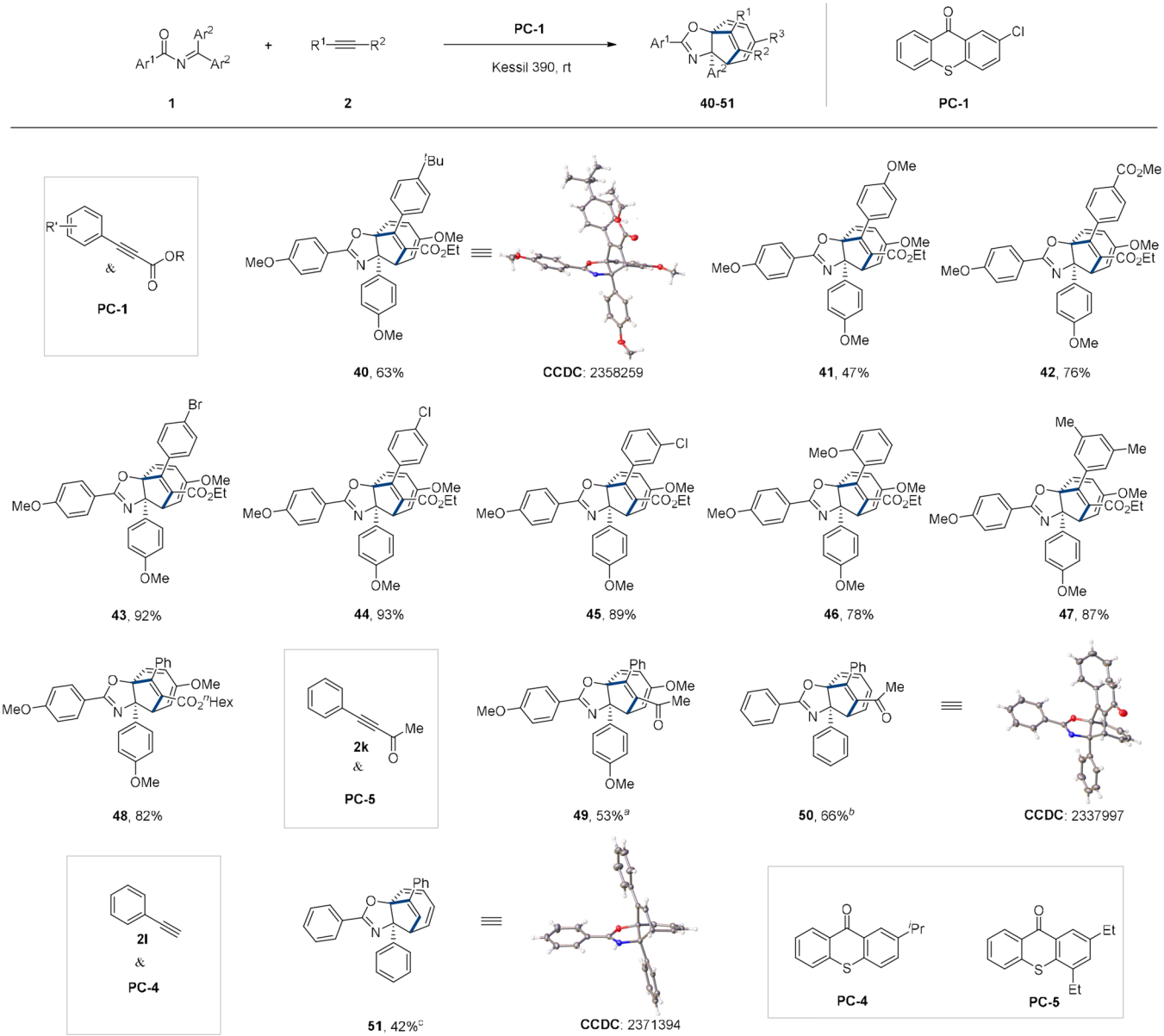

Figure 3. Substrate scope of the alkynes. Conditions: **1t** (0.20 mmol), **2** (0.50 mmol), **PC-1** (0.04 mmol), $ZnCl_2$ (0.20 mmol), MeCN (0.5 mL), Kessil 390 nm, 40 W, rt, 24 h; [a]**2k** (0.60 mmol), **PC-5** (0.03 mmol), MeCN (1.0 mL), Kessil 390 nm, 40 W, rt, 24 h; [b]**1a** (0.20 mmol), **2k** (0.50 mmol), **PC-5** (0.03 mmol), $Mn(OAc)_2$ (0.20 mmol), MeCN (2.0 mL), 390 nm, 100 W, rt, 24 h; [c]**2l** (1.0 mmol), **PC-4** (0.03 mmol), $ZnCl_2$ (0.20 mmol), ^{i}PrOH (1.0 mL), 390 nm, 50 W, rt, 24 h; isolated yields were given in all cases.

additives and the concentration of the reaction had slightly unfavorable effects on the yields (entry 11, Table S1 and Tables S6 and S7 in the Supporting Information). The presence of a photocatalyst and light irradiation were essential in this reaction (entries 12 and 13, Table S1).

Substrate Scope. With the optimal conditions in hand, we systematically explored the substrate scope of this dearomative skeletal editing approach (Figure 2). A wide range of *N*-acylimines all proceeded smoothly, delivering the corresponding polycyclic frameworks with excellent chemo- and regioselectivities. For the aromatic ring (R = Ar^1) conjugated with the carbonyl group, a series of functional groups, including OMe (**4**, **7**, **9**), bromo (**5**), ester (**6**), and chloro (**8**, **10**, **11**), were well accommodated irrespective of their substituent positions, providing good opportunities for further transformations. Meanwhile, the robustness of this protocol was demonstrated by its compatibility with other (hetero)aromatic groups (**12**–**14**). Naphthyl (**12**) and thienyl (**13**) groups, which are typically influenced by EnT, remained unaffected under the conditions of this protocol. Notably, the pyridyl group also exhibited good compatibility (**14**), enabling the construction of a potentially novel pyridine−oxazoline-type ligand in one step. The structural variety of the ligand could be further enriched by changing the substituents of pyridines and subsequent modifications of the products. The alkyl group could also be applied to this reaction when stronger UV light irradiation was used (**15**), which further expanded the scope of this reaction.

Next, a series of aromatic rings (Ar^2) associated with the imine moiety were investigated under the standard conditions (Figure 2). Gratifyingly, modifying the position of aromatic ring substituents enabled the selective introduction of different

https://doi.org/10.1021/jacs.5c01983
J. Am. Chem. Soc. 2025, 147, 11533−11542

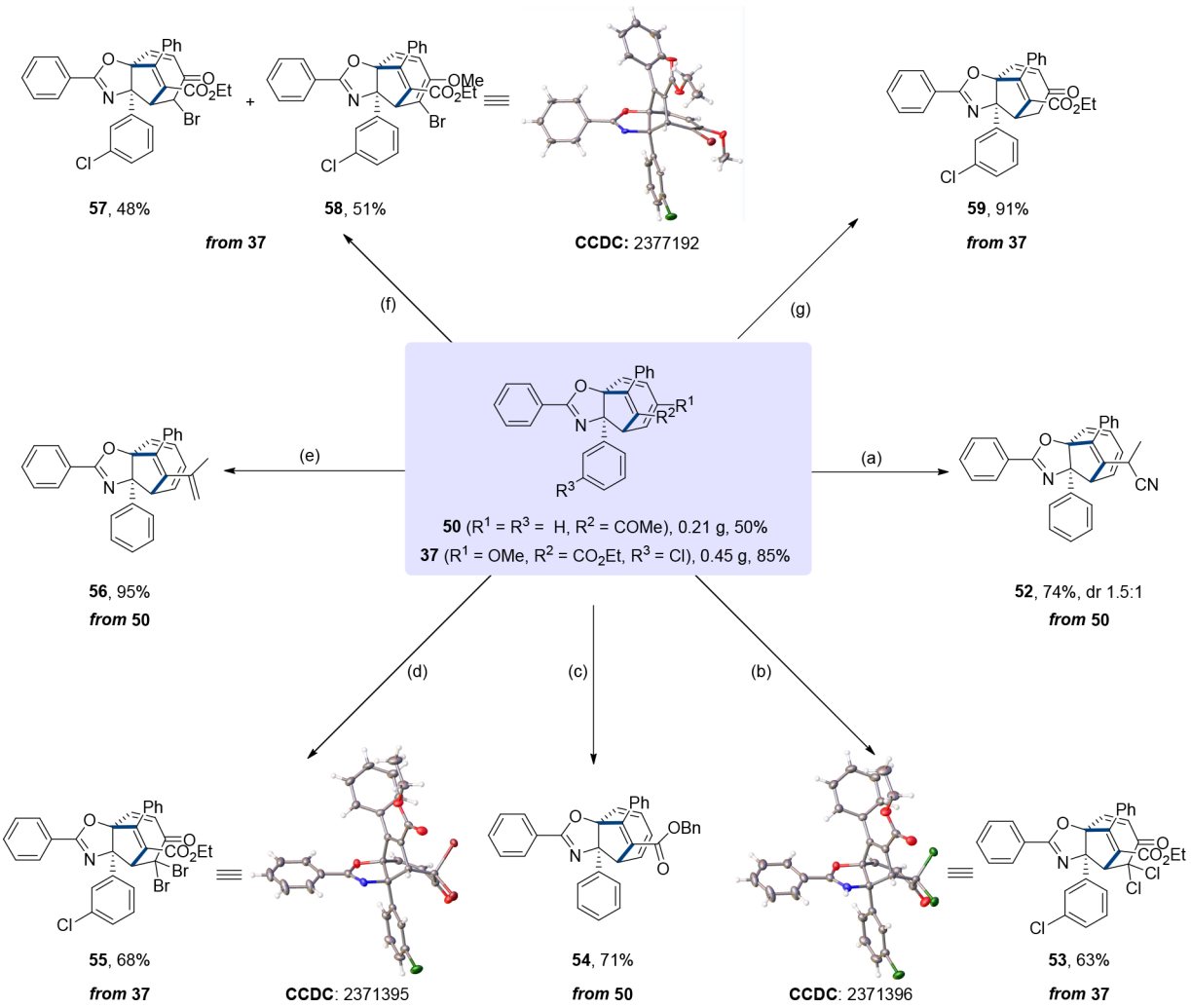

Figure 4. Synthetic derivatizations for constructing polyfunctional polycyclic structures. Conditions: (a) **50** (0.10 mmol), TosMIC (0.15 mmol), ^{t}BuOK (0.25 mmol), DME (0.6 mL), ^{t}BuOH (0.2 mL), 0 °C to rt, 6 h; (b) **37** (0.10 mmol), NCS (0.20 mmol), $Sc(OTf)_3$ (0.10 mmol), DCM (1.0 mL), rt, 18 h; (c) **50** (0.10 mmol), I_2 (0.30 mmol), DBU (0.40 mmol), BnOH (0.11 mmol), DCM (1.0 mL), 0 °C to rt, 16 h; (d) **37** (0.10 mmol), NBS (0.20 mmol), $Sc(OTf)_3$ (0.10 mmol), DCM (1.0 mL), rt, 18 h; (e) **50** (0.10 mmol), $MePPh_3Br$ (0.36 mmol), ^{t}BuOK (0.40 mmol), THF (1.0 mL), 0 °C to rt, 12 h; (f) **37** (0.10 mmol), $CuBr_2$ (0.20 mmol), DCM (0.5 mL), 70 °C, 12 h; (g) **37** (0.10 mmol), MeOH (0.13 mmol), TFA (0.5 mL), DCM (1.0 mL), 70 °C, 8 h.

substituents into distinct positions of conjugated dienes within seven-membered rings (**16**−**22**). For example, adjustment of the methyl group position on the aromatic ring (*ortho*, *meta*, and *para*) enabled predictable incorporation into specific positions of the seven-membered ring moiety (**16**, **20**, **20′**, and **22**). Similarly, methoxy-substituted conjugated diene units were efficiently assembled (**17**), enabling the rapid construction of multifunctionalized tropilene derivatives. Notably, halogenated conjugated diene structural units, which are challenging to construct, could also be accessed using this protocol (**18**, **19**, **21**, and **21′**). The presence of the OMe group on Ar^2 could generally give better performance. Moderate to high yields could be obtained for *N*-acylimines bearing electron-donating and -withdrawing substituents on the aromatic ring Ar^1 (**23**−**31**). This further expanded the structural diversity and functional group variety, facilitating the subsequent construction of diverse polycyclic structures. Furthermore, for unsymmetric imines, the selective dearomative skeletal editing of one of the aromatic rings Ar^2 was implemented smoothly (**32**−**37**). Substrates bearing a single substituent, either *para*-methoxy (**32**), *meta*-chloro (**34**), or *ortho*-methyl (**35**), selectively yielded their respective products with high regio-selectivities. For the *para*-chloro substrate, the reaction predominantly proceeded via the dearomative skeletal editing of the nonsubstituted aromatic ring (**33**). Notably, two different substituents could be simultaneously introduced into conjugated diene structures (**36**). For different aromatic rings containing substituents with varying properties, selective destruction of the aromaticity of one of the aromatic rings could also be achieved efficiently (**37**). The selective dearomative skeletal editing of the benzene ring could be achieved when one of the aromatic rings was replaced by a pyridyl moiety (**3aa**, Figure S14). When enones (**1aj** and **1ak**[14i]) were used instead of *N*-acylimines, no corresponding products were detected (**38** and **39**). The observed limitations may arise from the inherent challenges in substrate activation and the inability to mediate the radical [6+2] cycloaddition process (Tables S21 and S22). It indicated that the introduction of the nitrogen atom in the substrate is crucial for this protocol. The assignment of chemo-, regio- and stereoselectivities of this protocol was determined by crystal analysis of representative products **18**, **35**−**37**.

https://doi.org/10.1021/jacs.5c01983
J. Am. Chem. Soc. 2025, 147, 11533−11542

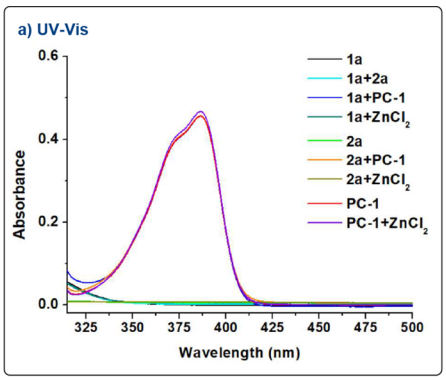

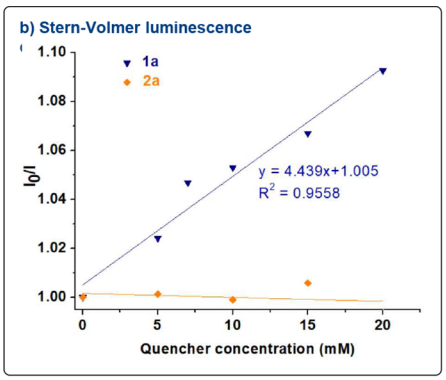

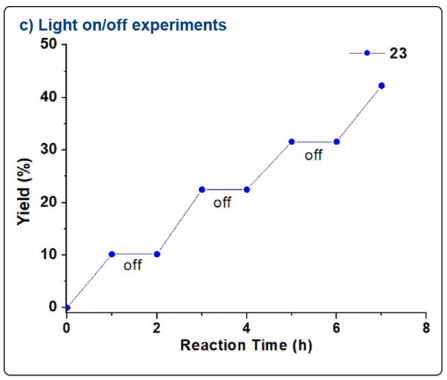

d) Intermediate capture experiment

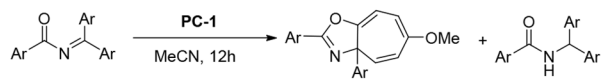

1t (Ar = PMP) 59%, rsm **60**, 34% **61**, 7%

e) Direct excitation experiment

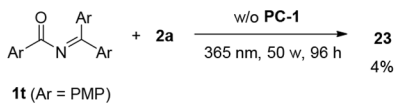

1t (Ar = PMP) **23** 4%

61 via diradical A

23 via diradical B

f) Intermediate conversion experiments

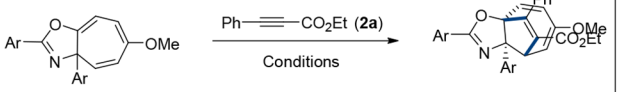

60 **23** (Ar = PMP)

Entry	Conditions	Yield of **1t**	Yield of **23**
1	**PC-1**, MeCN, 12 h	N.D.	60%
2	w/o **PC-1**, MeCN, 12 h	N.D.	N.D.
3	**PC-1**, dark, 70 °C, 12 h	86%	N.D.

g) Comparison of various triplet photocatalysts

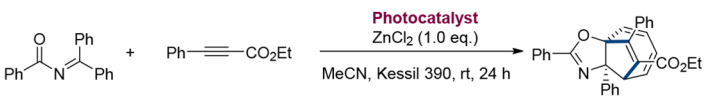

1a **2a** **3**

Entry	PC (2.0 mol%)	$E_{1/2}(PC^+/PC^*)$	$E_{1/2}(PC^*/PC^-)$	E_T (kcal/mol)	Yield of **3**
1	---	---	---	---	---
2	[Mes-Acr](ClO_4)	---	+2.81 V	44.7	---
3	[Ru(bpy)$_3$](BF_4)$_2$	-0.81 V	+0.77 V	49.2	---
4	*fac*-[Ir(bpy)$_3$]	-1.73 V	+0.31 V	58.1	---
5	[Ir(dF(CF_3)ppy)$_2$(dtbbpy)]PF_6	-0.89 V	+1.21 V	61.8	21%
6	TXT (PC-2) (20 mmol%)	-1.11 V	+1.18 V	63.4	56%

increasing triplet-state energy

h) Kinetic studies

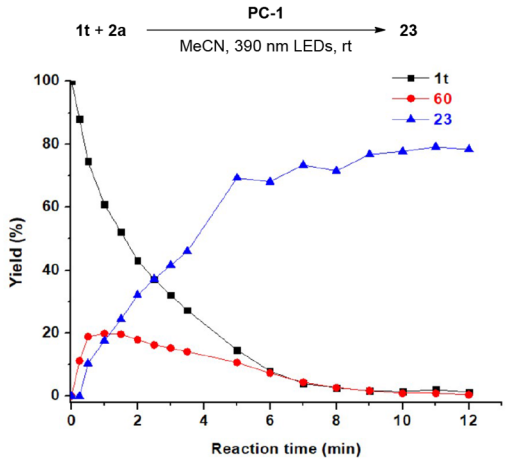

i) Radical inhibition experiments

1t (Ar = PMP) **2a** **23**

Entry	Additives	Yield of **23**
1	TEMPO	N.D.
2	DMPO	N.D.
3	BHT	20%
4	Air	7%
5	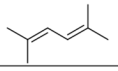	N.D.

j) Radical capture experiments

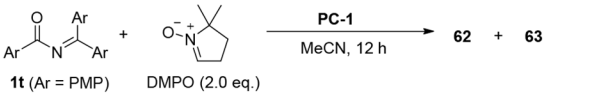

1t (Ar = PMP) DMPO (2.0 eq.)

Entry	Conditions	Yield of **62**	Yield of **63**
1	with $ZnCl_2$	22%	12%
2	w/o $ZnCl_2$	13%	22%

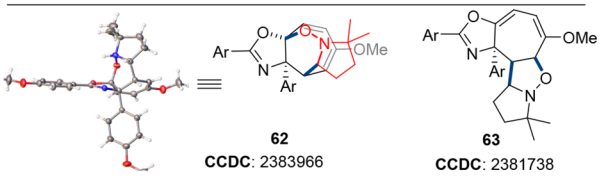

62 **CCDC**: 2383966 **63** **CCDC**: 2381738

Figure 5. Mechanism experiments.

https://doi.org/10.1021/jacs.5c01983
J. Am. Chem. Soc. 2025, 147, 11533−11542

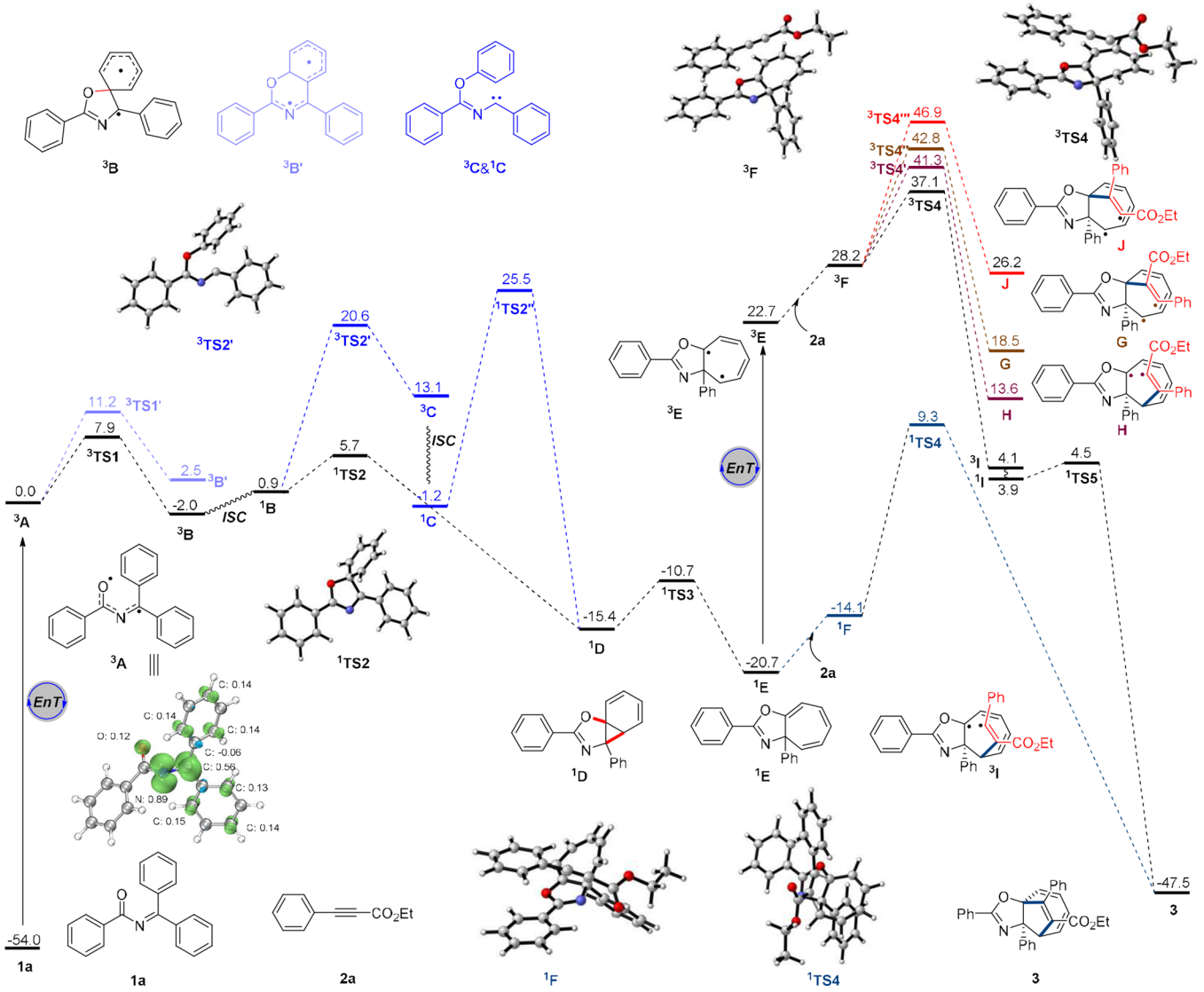

Figure 6. Reaction energy profiles for the dearomative skeletal editing of benzenoids.

To expand the application range of substrates, subsequently, a series of alkynes were evaluated (Figure 3). Fortunately, a wide range of different substituted phenylpropiolates could be well tolerated in this protocol irrespective of their electronic factors (**40**−**48**). The positional variation of the substituents had a minimal effect on the reaction (**41** vs **46**, **44** vs **45**). By slightly changing the reaction conditions, the applicability of the reaction was further extended. 4-Phenylbut-3-yn-2-one containing both alkynyl and carbonyl groups that are susceptible to an energy transfer catalytic reaction was also compatible with this method (**49** and **50**). Besides, simple phenylacetylene could be well accommodated in this protocol (**51**). Moreover, methyl propiolate was also tolerated under the conditions (**3ac**, Figure S14). The resulting trisubstituted alkenes were preserved under the reaction conditions without undergoing further side reactions.

In order to demonstrate the comprehensive utility of the protocol, various transformations were performed (Figure 4). Scale-up reactions for representative compounds **37** and **50** were successfully performed following this protocol, demonstrating its effectiveness and reproducibility on a larger scale. For product **50** containing a methyl ketone structure, the conversion of the carbonyl to cyano group was achieved through the Van Leusen reaction (**52**). Taking advantage of enol isomerization, a polycyclic skeleton containing tropilene structural units could be synthesized with **37** serving as the substrate (**53**, **55**, **57**−**59**). Remarkably, two halogen (Cl or Br) substituents could also be introduced into the α position of the carbonyl group at the same time with the addition of electrophiles (**53** and **55**). A conjugated diene unit containing both Br and OMe was constructed by electrophilic substitution (**58**), and an α-bromo-unsaturated ketone structure could be obtained by isomerization of enol (**57**). Furthermore, ketone-to-ester transformation was achieved by the haloform coupling reaction of **50** with benzyl alcohol (**54**). The polycyclic compound containing a polyene skeleton could be accessed via the Witting reaction (**56**). The assignment of the stereochemistry of products **53**, **55**, and **58** was further confirmed through single-crystal X-ray crystallography.

Mechanistic Investigations. To gain insight into the mechanistic underpinnings of this dearomative skeletal editing protocol, a series of mechanism experiments were performed (Figure 5). UV/vis spectroscopy of the reaction components revealed that **PC-1** was the only light-absorbing species around

https://doi.org/10.1021/jacs.5c01983
J. Am. Chem. Soc. 2025, 147, 11533−11542

a wavelength of 390 nm (Figure 5a). This result also excluded the possibility of the direct excitation of **1a** or **2a**, as well as the formation of a photoexcited EDA complex between **1a** and **2a**. In addition, Stern−Volmer quenching studies clearly demonstrated that **1a** and **60** quenched the excited photocatalyst (**PC-1***), while **2a** had no detectable quenching (Figures 5b and S10). Light on/off experiments indicated that irradiation of visible light was indispensable (Figure 5c). The corresponding Büchner reaction product **60** could be isolated in the absence of alkyne **2a** (Figure 5d). The side product **61** was probably formed through diradical A. The direct excitation experiment with stronger UV light (λ_{max} = 365 nm) of the standard reaction gave 4% yield after 96 h (Figure 5e). When the phenyl group was replaced by the benzyl group, no corresponding product was detected (Table S17), indicating that the reaction was probably initiated by the sensitization of the carbonyl group (via diradical B). When the intermediate **60** was employed in the reaction, it was found that the corresponding desired product **23** could be obtained only under standard conditions. It could not be obtained in the absence of a photocatalyst or only heating. On the contrary, the associated substrate **1t** was recovered under thermal conditions (Figure 5f).

Next, a series of photocatalysts with different triplet energies were tested (Figure 5g). The yields exhibited a general trend of increasing with the rise in triplet energy, while no relation was found with respect to the redox potentials. The kinetic experiments showed that the Büchner product **60** was predominantly generated in the first half hour and then gradually decreased with time. Meanwhile, the corresponding product **23** progressively increased over time (Figure 5h). Subsequently, a series of radical inhibition experiments were carried out (Figure 5i). The reaction was significantly or completely inhibited by adding a variety of free radical inhibitors (2,2,6,6-tetramethylpiperidinoxy, TEMPO; 5,5-dimethyl-1-pyrroline *N*-oxide, DMPO; butylated hydroxytoluene, BHT) to the reaction mixture. These results suggested a radical pathway was probably involved in this reaction. Meanwhile, in the presence of a triplet quencher (O_2 or 2,5-dimethylhexa-2,4 diene), the reaction was also greatly or completely inhibited, suggesting that the reaction was most likely mediated via EnT. Notably, in the presence of DMPO, a new compound with an $[M + H]^+$ of 489.2359 was detected (Figure S13). Therefore, radical trapping experiments were carried out (Figure 5j). When DMPO was used as the spin trapping reagent,[17] two interesting products (**62** and **63**) of the reaction of **1t** with DMPO could be isolated and verified by X-ray crystallography. It indicated that the reaction probably took place via a diradical intermediate.

Based on the aforementioned mechanistic studies and further DFT calculations, a plausible energy transfer mechanism is shown in Figure 6. Visible light excited PC sensitizes *N*-(diphenylmethylene) benzamide (**1a**) by EnT, which subsequently produces diradical ^{3}**A**. Then, the oxygen radical of ^{3}**A** attacks the benzene ring to produce the corresponding dearomatic diradical intermediate ^{3}**B** via ^{3}**TS1**. The spin density distribution of ^{3}**A** further rationalizes the formation of ^{3}**B**. The intersystem crossing of the generated triplet 1,3-diradical allows subsequent radical−radical recombination to produce the corresponding NCD intermediate ^{1}**D** via ^{1}**TS2** ($\Delta G_2^{\ddagger}$ = 4.8 kcal/mol). Moreover, the formation of ^{1}**D** via the generation of the corresponding carbene ^{3}**C** followed by the Büchner reaction is excluded (^{3}**TS2′**, $\Delta G_{2'}^{\ddagger}$ = 19.7 kcal/mol). Afterward, the NCD ^{1}**D** undergoes electrocyclization rearrangement to generate the CHT intermediate ^{1}**E**. Subsequently, the excited PC sensitizes ^{1}**E** by EnT and the resulting triplet state ^{3}**E** approaches ethyl 3-phenylpropiolate (**2a**) to form the exciplex ^{3}**F**. This exciplex results in the formation of the first C−C bond between ^{3}**E** and the alkyne **2a**, which determines the regioselectivity. Furthermore, the process of directly obtaining ^{3}**E** from sensitized ^{1}**D** is not feasible (via ^{3}**TS3**, $\Delta G_{3'}^{\ddagger}$ = 14.7 kcal/mol, Figure S15). DFT calculations disclose that the transition state in which the pure carbon radical of ^{3}**E** engages **2a** in the 2-position is thermodynamically the most favorable ($\Delta G_4^{\ddagger}$ = 8.9 kcal/mol), leading to the observed regioisomer. Other regional isomers are required to overcome higher free energy barriers, 13.1 kcal/mol (via ^{3}**TS4′**), 14.6 kcal/mol (via ^{3}**TS4″**), and 18.7 kcal/mol (via ^{3}**TS4‴**). The resulting intersystem crossing of the triplet 1,5-diradical allows subsequent *cis*-selective radical−radical recombination as a diastereoselective determining step, resulting in the final dearomative skeletal editing product **3**. Meanwhile, both theory and experiment excluded the possibility of the [6+2] cycloaddition of ^{1}**E** and **2a** in the ground state to obtain the target product **3** (via ^{1}**TS4**, $\Delta G^{1}{}_4^{\ddagger}$ = 23.4 kcal/mol).

CONCLUSIONS

In conclusion, a new strategy for the dearomative skeletal editing of benzenoids has been developed by smooth merging of the photoinduced dearomative skeletal editing with [6+2] cycloaddition. *N*-Acylimines serve as an atom-economic diradical precursor to generate the cycloheptatriene diradical under EnT. This strategy features excellent chemo-, regio-, and diastereoselectivities and broad functional group tolerance. A series of structurally diverse polycyclic frameworks can be obtained simply by modifying the substituents on the aromatic ring. The experimental and computational results indicate that the rapid iteration of multiple diradicals and their matching with alkynes is crucial for achieving the highly selective dearomatization and skeletal editing of benzenoids. Synthetic derivatizations further prove the practicability of the strategy.

ASSOCIATED CONTENT

Supporting Information

The Supporting Information is available free of charge at https://pubs.acs.org/doi/10.1021/jacs.5c01983.

Experimental procedures, characterization data, and NMR spectra (PDF)

Accession Codes

Deposition Numbers 2337997, 2358259, 2361517, 2365267−2365268, 2371394−2371396, 2377190, 2377192, 2381738, 2383966, and 2413146 contain the supplementary crystallographic data for this paper. These data can be obtained free of charge via the joint Cambridge Crystallographic Data Centre (CCDC) and Fachinformationszentrum Karlsruhe Access Structures service.

AUTHOR INFORMATION

Corresponding Author

Qing-An Chen − *Dalian Institute of Chemical Physics, Chinese Academy of Sciences, Dalian 116023, People's Republic of China; University of Chinese Academy of Sciences, Beijing 100049, People's Republic of China;*

https://doi.org/10.1021/jacs.5c01983
J. Am. Chem. Soc. 2025, 147, 11533−11542

orcid.org/0000-0002-9129-2656; Email: qachen@dicp.ac.cn; www.lbcs.dicp.ac.cn

Authors

Xiang-Xin Zhang − *Dalian Institute of Chemical Physics, Chinese Academy of Sciences, Dalian 116023, People's Republic of China; University of Chinese Academy of Sciences, Beijing 100049, People's Republic of China;* orcid.org/0000-0003-0897-5577

Shan-Tong Xu − *Dalian Institute of Chemical Physics, Chinese Academy of Sciences, Dalian 116023, People's Republic of China*

Xue-Ting Li − *Dalian Institute of Chemical Physics, Chinese Academy of Sciences, Dalian 116023, People's Republic of China; University of Chinese Academy of Sciences, Beijing 100049, People's Republic of China;* orcid.org/0009-0006-4290-5555

Ting-Ting Song − *Dalian Institute of Chemical Physics, Chinese Academy of Sciences, Dalian 116023, People's Republic of China*

Ding-Wei Ji − *Dalian Institute of Chemical Physics, Chinese Academy of Sciences, Dalian 116023, People's Republic of China*

Complete contact information is available at: https://pubs.acs.org/10.1021/jacs.5c01983

Notes

The authors declare no competing financial interest.

■ ACKNOWLEDGMENTS

Financial support from the National Natural Science Foundation of China (22371275) is acknowledged.

■ REFERENCES

(1) von Schleyer, P. R.; Jiao, H. What Is Aromaticity? *Pure Appl. Chem.* **1996**, *68*, 209−218.

(2) (a) Wang, C.-S.; Dixneuf, P. H.; Soulé, J.-F. Photoredox Catalysis for Building C−C Bonds from C(Sp2)−H Bonds. *Chem. Rev.* **2018**, *118*, 7532−7585. (b) Wang, H.; Gao, X.; Lv, Z.; Abdelilah, T.; Lei, A. Recent Advances in Oxidative R1-H/R2-H Cross-Coupling with Hydrogen Evolution Via Photo-/Electrochemistry. *Chem. Rev.* **2019**, *119*, 6769−6787. (c) Wang, J.; Dong, G. Palladium/Norbornene Cooperative Catalysis. *Chem. Rev.* **2019**, *119*, 7478−7528. (d) Shi, J.; Li, L.; Li, Y. O-Silylaryl Triflates: A Journey of Kobayashi Aryne Precursors. *Chem. Rev.* **2021**, *121*, 3892−4044. (e) Docherty, J. H.; Lister, T. M.; McArthur, G.; Findlay, M. T.; Domingo-Legarda, P.; Kenyon, J.; Choudhary, S.; Larrosa, I. Transition-Metal-Catalyzed C−H Bond Activation for the Formation of C−C Bonds in Complex Molecules. *Chem. Rev.* **2023**, *123*, 7692−7760. (f) Ali, W.; Oliver, G. A.; Werz, D. B.; Maiti, D. Pd-Catalyzed Regioselective Activation of C(Sp2)−H and C(Sp3)−H Bonds. *Chem. Soc. Rev.* **2024**, *53*, 9904−9953.

(3) (a) Lovering, F.; Bikker, J.; Humblet, C. Escape from Flatland: Increasing Saturation as an Approach to Improving Clinical Success. *J. Med. Chem.* **2009**, *52*, 6752−6756. (b) Lovering, F. Escape from Flatland 2: Complexity and Promiscuity. *MedChemComm* **2013**, *4*, 515−519.

(4) (a) Roche, S. P.; Porco, J. A. Dearomatization Strategies in the Synthesis of Complex Natural Products. *Angew. Chem., Int. Ed.* **2011**, *50*, 4068−4093. (b) Zhuo, C. X.; Zhang, W.; You, S. L. Catalytic Asymmetric Dearomatization Reactions. *Angew. Chem., Int. Ed.* **2012**, *51*, 12662−12686. (c) Wertjes, W. C.; Southgate, E. H.; Sarlah, D. Recent Advances in Chemical Dearomatization of Nonactivated Arenes. *Chem. Soc. Rev.* **2018**, *47*, 7996−8017. (d) Huck, C. J.; Sarlah, D. Shaping Molecular Landscapes: Recent Advances, Opportunities, and Challenges in Dearomatization. *Chem.* **2020**, *6*, 1589−1603. (e) Ji, P.; Duan, K.; Li, M.; Wang, Z.; Meng, X.; Zhang, Y.; Wang, W. Photochemical Dearomative Skeletal Modifications of Heteroaromatics. *Chem. Soc. Rev.* **2024**, *53*, 6600−6624. (f) Wiesenfeldt, M. P.; Nairoukh, Z.; Dalton, T.; Glorius, F. Selective Arene Hydrogenation for Direct Access to Saturated Carbo- and Heterocycles. *Angew. Chem., Int. Ed.* **2019**, *58*, 10460−10476. (g) Heravi, M.; Vazinfard, M.; Faghihi, Z. Recent Applications of Birch Reduction in Total Synthesis of Natural Products. *Curr. Org. Chem.* **2015**, *19*, 1491−1525. (h) Wu, W.-T.; Zhang, L.; You, S.-L. Catalytic Asymmetric Dearomatization (CADA) Reactions of Phenol and Aniline Derivatives. *Chem. Soc. Rev.* **2016**, *45*, 1570−1580. (i) Lan, P.; Ye, S.; Banwell, M. G. The Application of Dioxygenase-Based Chemoenzymatic Processes to the Total Synthesis of Natural Products. *Chem.—Asian J.* **2019**, *14*, 4001−4012. (j) Liebov, B. K.; Harman, W. D. Group 6 Dihapto-Coordinate Dearomatization Agents for Organic Synthesis. *Chem. Rev.* **2017**, *117*, 13721−13755. (k) Sarlah, D.; Okumura, M. Arenophile-Mediated Dearomative Functionalization Strategies. *Synlett* **2018**, *29*, 845−855.

(5) (a) Streit, U.; Bochet, C. G. The Arene−Alkene Photocycloaddition. *Beilstein J. Org. Chem.* **2011**, *7*, 525−542. (b) Remy, R.; Bochet, C. G. Arene−Alkene Cycloaddition. *Chem. Rev.* **2016**, *116*, 9816−9849.

(6) Bird, C. W. The Relationship of Classical and Magnetic Criteria of Aromaticity. *Tetrahedron* **1996**, *52*, 9945−9952.

(7) (a) Strieth-Kalthoff, F.; James, M. J.; Teders, M.; Pitzer, L.; Glorius, F. Energy Transfer Catalysis Mediated by Visible Light: Principles, Applications, Directions. *Chem. Soc. Rev.* **2018**, *47*, 7190−7202. (b) Großkopf, J.; Kratz, T.; Rigotti, T.; Bach, T. Enantioselective Photochemical Reactions Enabled by Triplet Energy Transfer. *Chem. Rev.* **2022**, *122*, 1626−1653. (c) Strieth-Kalthoff, F.; Glorius, F. Triplet Energy Transfer Photocatalysis: Unlocking the Next Level. *Chem.* **2020**, *6*, 1888−1903.

(8) (a) Palai, A.; Rai, P.; Maji, B. Rejuvenation of Dearomative Cycloaddition Reactions via Visible Light Energy Transfer Catalysis. *Chem. Sci.* **2023**, *14*, 12004−12025. (b) Saha, D. Catalytic Dearomative Cycloaddition Reactions Enabled by Visible Light. *Asian J. Org. Chem.* **2024**, *13*, No. e202400374.

(9) Cornelisse, J. The Meta Photocycloaddition of Arenes to Alkenes. *Chem. Rev.* **1993**, *93*, 615−669.

(10) (a) Ma, J. J.; Chen, S. M.; Bellotti, P.; Guo, R. Y.; Schäfer, F.; Heusler, A.; Zhang, X. L.; Daniliuc, C.; Brown, M. K.; Houk, K. N.; Glorius, F. Photochemical Intermolecular Dearomative Cycloaddition of Bicyclic Azaarenes with Alkenes. *Science* **2021**, *371*, 1338−1345. (b) Guo, R.; Adak, S.; Bellotti, P.; Gao, X.; Smith, W. W.; Le, S. N.; Ma, J.; Houk, K. N.; Glorius, F.; Chen, S.; Brown, M. K. Photochemical Dearomative Cycloadditions of Quinolines and Alkenes: Scope and Mechanism Studies. *J. Am. Chem. Soc.* **2022**, *144*, 17680−17691. (c) Ma, J.; Chen, S.; Bellotti, P.; Wagener, T.; Daniliuc, C.; Houk, K. N.; Glorius, F. Facile Access to Fused 2d/3d Rings via Intermolecular Cascade Dearomative [2 + 2] Cycloaddition/Rearrangement Reactions of Quinolines with Alkenes. *Nat. Catal.* **2022**, *5*, 405−413. (d) Kleinmans, R.; Dutta, S.; Ozols, K.; Shao, H.; Schäfer, F.; Thielemann, R. E.; Chan, H. T.; Daniliuc, C. G.; Houk, K. N.; Glorius, F. Ortho-Selective Dearomative [$2\pi + 2\sigma$] Photocycloadditions of Bicyclic Aza-Arenes. *J. Am. Chem. Soc.* **2023**, *145*, 12324−12332. (e) Dutta, S.; Lee, D.; Ozols, K.; Daniliuc, C. G.; Shintani, R.; Glorius, F. Photoredox-Enabled Dearomative [$2\pi + 2\sigma$] Cycloaddition of Phenols. *J. Am. Chem. Soc.* **2024**, *146*, 2789−2797.

(11) (a) Zhu, M.; Zhang, X.; Zheng, C.; You, S.-L. Energy-Transfer-Enabled Dearomative Cycloaddition Reactions of Indoles/Pyrroles via Excited-State Aromatics. *Acc. Chem. Res.* **2022**, *55*, 2510−2525. (b) Li, M.; Huang, X.-L.; Zhang, Z.-Y.; Wang, Z.; Wu, Z.; Yang, H.; Shen, W.-J.; Cheng, Y.-Z.; You, S.-L. Gd(III)-Catalyzed Regio-, Diastereo-, and Enantioselective [4 + 2] Photocycloaddition of Naphthalene Derivatives. *J. Am. Chem. Soc.* **2024**, *146*, 16982−16989.

(12) (a) Jurczyk, J.; Woo, J.; Kim, S. F.; Dherange, B. D.; Sarpong, R.; Levin, M. D. Single-Atom Logic for Heterocycle Editing. *Nat. Synth.* **2022**, *1*, 352−364. (b) Joynson, B. W.; Ball, L. T. Skeletal

Editing: Interconversion of Arenes and Heteroarenes. *Helv. Chim. Acta* **2023**, *106*, No. e202200182. (c) Liu, Z.; Sivaguru, P.; Ning, Y.; Wu, Y.; Bi, X. Skeletal Editing of (Hetero)Arenes Using Carbenes. *Chem.—Eur. J.* **2023**, *29*, No. e202301227. (d) Liu, Z.; Zhang, X.; Sivaguru, P.; Bi, X. Triftosylhydrazone in Single-Atom Skeletal Editing. *Acc. Chem. Res.* **2025**, *58*, 130−149.

(13) Shi, C.-Y.; Zhu, G.-Y.; Xu, Y.; Teng, M.-Y.; Ye, L.-W. Recent Advances in Catalytic Asymmetric Büchner Reaction. *Chin. Chem. Lett.* **2023**, *34*, No. 108441.

(14) (a) Clayden, J.; Knowles, F. E.; Menet, C. J. Stereospecific Photochemical Ring Expansion of Lithiated Benzamides. *J. Am. Chem. Soc.* **2003**, *125*, 9278−9279. (b) Zeng, Q.; Dong, K.; Huang, J.; Qiu, L.; Xu, X. Copper-Catalyzed Carbene/Alkyne Metathesis Terminated with the Buchner Reaction: Synthesis of Dihydrocyclohepta[b]-Indoles. *Org. Biomol. Chem.* **2019**, *17*, 2326−2330. (c) Mykura, R.; Sánchez-Bento, R.; Matador, E.; Duong, V. K.; Varela, A.; Angelini, L.; Carbajo, R. J.; Llaveria, J.; Ruffoni, A.; Leonori, D. Synthesis of Polysubstituted Azepanes by Dearomative Ring Expansion of Nitroarenes. *Nat. Chem.* **2024**, *16*, 771−779. (d) Patel, S. C.; Burns, N. Z. Conversion of Aryl Azides to Aminopyridines. *J. Am. Chem. Soc.* **2022**, *144*, 17797−17802. (e) Mailloux, M. J.; Fleming, G. S.; Kumta, S. S.; Beeler, A. B. Unified Synthesis of azepines by Visible-Light-Mediated Dearomative Ring Expansion of Aromatic N-Ylides. *Org. Lett.* **2021**, *23*, 525−529. (f) Ito, T.; Harada, S.; Homma, H.; Takenaka, H.; Hirose, S.; Nemoto, T. Asymmetric Intramolecular Dearomatization of Nonactivated Arenes with Ynamides for Rapid Assembly of Fused Ring System under Silver Catalysis. *J. Am. Chem. Soc.* **2021**, *143*, 604−611. (g) Wang, X.; Abrahams, Q. M.; Zavalij, P. Y.; Doyle, M. P. Highly Regio- and Stereoselective Dirhodium Vinylcarbene Induced Nitrone Cycloaddition with Subsequent Cascade Carbenoid Aromatic Cycloaddition/N-O Cleavage and Rearrangement. *Angew. Chem., Int. Ed.* **2012**, *51*, 5907−5910. (h) Xia, J.; Liu, J.; Yu, Y.; Zhang, J.; Huang, X. Divergent Access to Polycyclic N-Heterocyclic Compounds through Büchner-Type Dearomatization Enabled Cycloisomerization of Diynamides under Gold Catalysis. *Org. Lett.* **2022**, *24*, 4298−4303. (i) Zhang, L.; You, M.; Ban, X.; Zhao, X.; Yin, Y.; Cao, S.; Jiang, Z. Visible Light-Driven Dearomative Ring Expansion of (Aza)Arenes to Access Dihydrofuran-Based Polycyclic Compounds. *Chem. Sci.* **2024**, *15*, 8828−8834. (j) Liu, Z.; Tan, H.; Wang, L.; Fu, T.; Xia, Y.; Zhang, Y.; Wang, J. Transition-Metal-Free Intramolecular Carbene Aromatic Substitution/Büchner Reaction: Synthesis of Fluorenes and [6,5,7]Benzo-Fused Rings. *Angew. Chem., Int. Ed.* **2015**, *54*, 3056−3060. (k) Harada, S.; Takenaka, H.; Ito, T.; Kanda, H.; Nemoto, T. Valence-Isomer Selective Cycloaddition Reaction of Cycloheptatrienes-Norcaradienes. *Nat. Commun.* **2024**, *15*, 2309. (l) Li, H.; Li, N.; Wu, J.; Yu, T.; Zhang, R.; Xu, L.-P.; Wei, H. Rhodium-Catalyzed Intramolecular Nitrogen Atom Insertion into Arene Rings. *J. Am. Chem. Soc.* **2023**, *145*, 17570−17576.

(15) McNamara, O. A.; Maguire, A. R. The Norcaradiene−Cycloheptatriene Equilibrium. *Tetrahedron* **2011**, *67*, 9−40.

(16) (a) Guo, S.-Y.; Yang, F.; Song, T.-T.; Guan, Y.-Q.; Min, X.-T.; Ji, D.-W.; Hu, Y.-C.; Chen, Q.-A. Photo-Induced Catalytic Halopyridylation of Alkenes. *Nat. Commun.* **2021**, *12*, 6538. (b) Song, T. T.; Mei, Y. K.; Liu, Y.; Wang, X. Y.; Guo, S. Y.; Ji, D. W.; Wan, B.; Yuan, W.; Chen, Q. A. Construction of Bridged Benzazepines via Photo-Induced Dearomatization. *Angew. Chem., Int. Ed.* **2023**, *63*, No. e202314304. (c) Zhang, X.-X.; Zheng, H.; Mei, Y.-K.; Liu, Y.; Liu, Y.-Y.; Ji, D.-W.; Wan, B.; Chen, Q.-A. Photo-Induced Imino Functionalizations of Alkenes via Intermolecular Charge Transfer. *Chem. Sci.* **2023**, *14*, 11170−11179. (d) Guo, S.-Y.; Liu, Y.-P.; Huang, J.-S.; He, L.-B.; He, G.-C.; Ji, D.-W.; Wan, B.; Chen, Q.-A. Visible Light-Induced Chemoselective 1,2-Diheteroarylation of Alkenes. *Nat. Commun.* **2024**, *15*, 6102.

(17) Janzen, E. G. Spin Trapping. *Acc. Chem. Res.* **1971**, *4*, 31−40.

https://doi.org/10.1021/jacs.5c01983
J. Am. Chem. Soc. 2025, 147, 11533−11542